A Technique for Extending the Dynamic Range of the Dual Six-Port Network Analyzer

JOHN R. JUROSHEK AND CLETUS A. HOER, MEMBER, IEEE

Abstract — **The dynamic range of the six-port type of automatic network analyzer is typically limited to measuring two-port devices with a transmission coefficient S_{12} in the range of 0 to −60 dB. The following describes a subcarrier approach for extending the dynamic range of the dual six-port network analyzer. The subcarrier is generated by inserting a 10-kHz, biphase modulator ahead of one of the six-ports. With the subcarrier approach, measurements of S_{12} in the range of −60 to −100 dB can be made. Test results are presented showing measurements of $S_{12} = -80$ db with a precision of ±0.05 dB or better, and an accuracy of ±0.16 dB or better at 3 GHz. Measurement results are also presented showing the dynamic range achievable with thermistor and barretter detectors.**

Key Words: **barretter power detectors; diode power detectors; impedance measurements; microwave network analyzer; six-port network analyzer; thermistor power detectors.**

I. Introduction

ONE OF THE disadvantages of the six-port type of automatic network analyzer is its limited dynamic range. Six-ports are typically limited to measuring two-port devices with S_{12} in the range of 0 to 60 dB [1]. The reason for this limitation is the limited dynamic range of the thermistors and diode power detectors commonly used in these analyzers.

The following describes a subcarrier approach for extending the dynamic range of a dual six-port network analyzer. With this technique, measurements of S_{12} in the range of −60 to −100 dB can be made. Test results are presented showing measurements of $S_{12} = -80$ dB with a precision of ±0.05 dB or better and an accuracy of ±0.16 dB or better at 3 GHz. The frequency of the subcarrier in these tests is 10 kHz. The 10-kHz signal is detected with a coherent vector voltmeter (lock-in amplifier). Measurement results are presented showing the dynamic range achievable with thermistor, barretter, and zero-bias, low-barrier Schottky-diode detectors.

II. Theory

Consider the arrangement shown in Fig. 1 with a dual six-port network analyzer, a device under test (DUT), and a 0 to 180° phase shifter. The complex waveforms a_1, b_1, a_2, and b_2 are defined as shown in the figure. Let the scattering equations for the two-port under test when the phase shifter is in the 0° position be

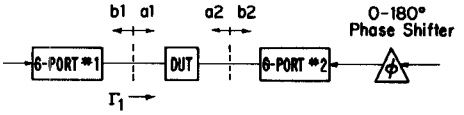

Fig. 1. Block diagram defining waveforms into the device under test.

$$b_1 = S_{11}a_1 + S_{12}a_2 \tag{1}$$

$$b_2 = S_{21}a_1 + S_{22}a_2. \tag{2}$$

From (1), the reflection coefficient Γ_1 measured at port 1 is

$$\Gamma_1 = \frac{b_1}{a_1} = S_{11} + S_{12}\frac{a_2}{a_1}. \tag{3}$$

When the phase shifter is in the 180° position, (3) becomes

$$\Gamma_1' = S_{11} + S_{12}\frac{a_2'}{a_1'} \tag{4}$$

where the primes indicate values corresponding to the 180° setting of the phase shifter. The change in reflection coefficient $\Delta\Gamma_1$ at port 1 is obtained from (3) and (4)

$$\Gamma_1 - \Gamma_1' = S_{12}\left(\frac{a_2}{a_1} - \frac{a_2'}{a_1'}\right)$$

or

$$\Delta\Gamma_1 = S_{12}\Delta\phi \tag{5}$$

where $\Delta\phi$ is the change in a_2/a_1. It is shown in Appendix A that for high-loss pads (small $|S_{12}|$) which are reasonably well matched (small $|S_{11}|$ and $|S_{22}|$), $\Delta\phi$ is essentially a constant independent of the S-parameters of the device under test.

If the measurement system is symmetrical in arms 1 and 2 for the 0° phase position, and if the phase shifter is ideal with 180° phase change, $\Delta\phi = 2$ so that (5) becomes

$$S_{12} = \frac{\Delta\Gamma_1}{2} \qquad \text{(ideal case)}. \tag{6}$$

Equation (5) or (6) shows that S_{12} can be measured by a single reflectometer, and that the ability to measure small values of $|S_{12}|$ is determined by the resolution of the reflectometer (not necessarily a six-port) in measuring small *changes* in Γ. It is this feature that this paper attempts to exploit.

Manuscript received June 10, 1984; revised January 14, 1985. This work was supported in part by the Calibration Coordination Group of the Department of Defense.

The authors are with the National Bureau of Standards, Boulder, CO 80303.

It has been shown that in general for any six-port [2]

$$\Gamma_1 = \frac{1}{|a_1|^2} \sum_{i=1}^{4} C_i P_i \tag{7}$$

where P_i is the power absorbed by the detector on port i, and C_i are complex constants which are determined by the six-port calibration process [2]. Assuming that $|a_1|$ remains constant for the two positions of the phase shifter, (7) gives

$$\Delta\Gamma_1 = \frac{1}{|a_1|^2} \sum_{i=1}^{4} C_i \Delta P_i \tag{8}$$

where ΔP_i is the change in power at sidearm i corresponding to the two positions of the phase shifter.

It has also been shown from six-port theory that

$$|a_1|^2 = \sum_{i=1}^{4} \alpha_i P_i \tag{9}$$

where the α_i are real constants determined by the six-port calibration process. Let the output of sidearm 4 be proportional mainly to the incident wave a_1, and write (9) as

$$|a_1|^2 = P_4 \sum_{i=1}^{4} \alpha_i P_i / P_4$$

$$= P_4 \alpha. \tag{10}$$

It is shown in Appendix B that α is essentially a constant when measuring high-loss pads which are reasonably well matched. Since P_4 does not change as the phase shifter is switched, $\Delta P_4 = 0$ in (8). Combining (10), (8), and (5) gives

$$S_{12} = \frac{\Delta\Gamma_1}{\Delta\phi} = \frac{\sum_{i=1}^{3} C_i \Delta P_i}{\alpha P_4 \Delta\phi}. \tag{11}$$

Note that S_{12} is determined by measuring a power change ΔP_i caused by a 0 to 180° phase shift. How one goes about measuring this power change can be significant. In the current generation of six-ports, this power change would be measured by slowly (switching rate $\leqslant$10 Hz) changing the phase shifter and making dc measurements of either the voltage or current to determine the power at each detector. However, if the phase is electronically switched, say at a 10-kHz rate, then the power can be measured with an ac device such as a vector voltmeter. A significant improvement in the detector dynamic range can be achieved with the latter method. Experiments by King [3] achieved a dynamic range of 109 dB at 4.89 GHz, with a biased Schottky diode, and a detection frequency of 10 kHz. In contrast, the dynamic range of these diodes, as used in the six-ports with the dc method of detection is only of the order of 80 dB. The improvement is due to the fact that with the dc detection method the detector noise is dominated by 1/f noise, while at 10 kHz the noise is primarily thermal and shot noise [3]. The following describes the dynamic range achievable on three different types of detectors using the subcarrier technique.

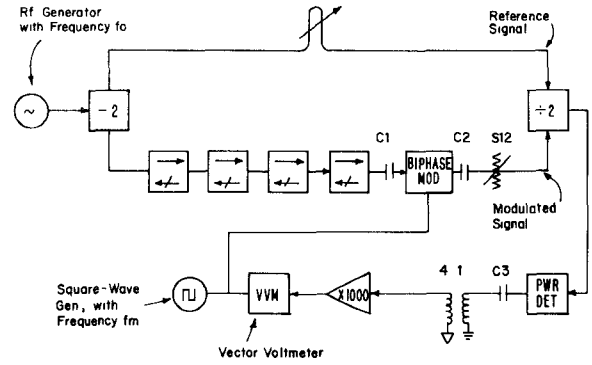

Fig. 2. Block diagram of test setup used to measure dynamic range of individual power detectors.

III. Detector Dynamic Range Measurements

The dynamic range of three different types of RF power detectors was measured using the arrangement shown in Fig. 2. In this test setup, the signal from the RF generator is divided into two paths. One half of the signal (reference signal) is sent through a length of line whose electrical length is adjustable. The remaining signal is sent through four isolators, a bi-phase modulator, and an adjustable attenuator. The reference and modulated signal are then summed and the resultant signal is sent to a power detector. The electrical length of the reference path is adjusted so that the reference and modulated signals add either in phase or 180° out of phase.

If the complex reference signal is denotated as r_1 and the complex modulated signal m_1, then the detector output, assuming a square-law detector, is given by the "law of cosines" as

$$k|r_1 + m_1|^2 = k\left[|r_1|^2 + |m_1|^2 - 2|r_1||m_1|\cos\alpha\right] \tag{12}$$

where k is the detector conversion constant, and α is the angle between r_1 and m_1. However, since α is either 0 or 180° depending on the modulator state, the detector output is

$$k|r_1 + m_1|^2 = k\left[|r_1|^2 + |m_1|^2 - 2|r_1||m_1|u(t)\right] \tag{13}$$

where $u(t)$ is a square wave of unity amplitude and frequency f_m. The dc terms in (13) are removed by capacitor C3, and the square wave

$$s(t) = -2k|r_1||m_1|u(t) \tag{14}$$

is sent to the 1:4 step-up transformer. The voltage of the fundamental frequency component of $s(t)$ after amplification in a low-noise preamplifier with a gain of 1000 is measured by the vector voltmeter.

The 1:4 step-up transformer along with capacitors C1 and C2 are primarily used to remove audio frequency ground loops. Capacitors C1 and C2 are inner and outer dc blocks, which means that the grounds for the RF generator, isolators, and power detector are dc isolated from the grounds for the bi-phase modulator, audio generator, and vector voltmeter.

Measurements were made on three different types of RF power detectors: a zero-bias, low-barrier Schottky diode; a

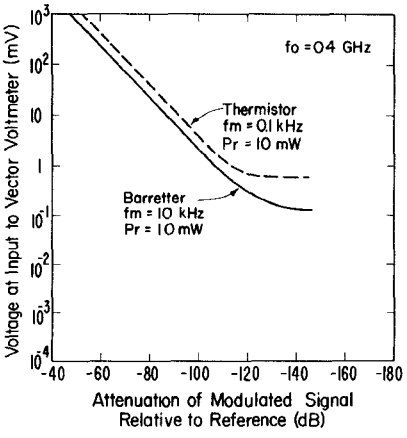

Fig. 3. Voltage at input to vector voltmeter versus attenuation of modulated signal relative to reference signal for thermistor and barretter.

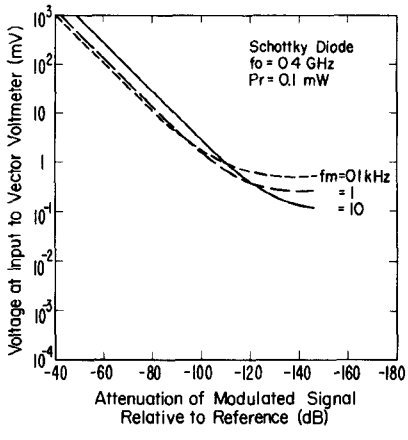

Fig. 4. Voltage at input to vector voltmeter versus attenuation of modulated signal relative to reference signal for Schottky diode.

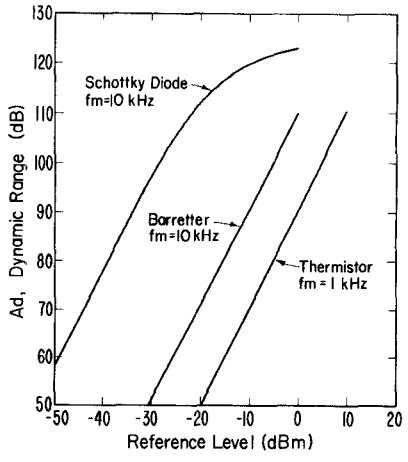

Fig. 5. Dynamic range of power detectors versus reference power level.

TABLE I
SUMMARY OF THE DYNAMIC RANGE *Ad* THAT WAS ACHIEVED USING THE SUBCARRIER MODULATION TECHNIQUE

f_0 (GHz)	f_m (kHz)	A_d (dB)	Comments
0.4	10	134	Schottky diode
	1	121	
	0.1	112	
2	10	120	
0.4	1	118	Thermistor
2		111	
0.4	10	130	Barretter
2		111	

The RF frequency is f_0 and modulation frequency is f_m.

thermistor; and a barretter. The thermistor and barretter were tested with the power meters that they are normally configured with for six-port applications. The thermistor is connected to a self-balancing power meter [4], while the barretter is connected to an NBS type-II power bridge [5]. The frequency response of the thermistor and self-balancing bridge is 1.6 kHz (3-dB cutoff frequency), and 17 kHz for the barretter and type-II bridge. It should be noted that these frequency responses are for the small (millivolt) signals encountered in this study.

The RF frequencies of 0.4 and 2 GHz were arbitrarily chosen for detector dynamic range measurements. Fig. 3 shows a typical result where the voltage at the input to the vector voltmeter is plotted as a function of the modulated signal level. The level of the modulated signal is expressed in decibels relative to the reference signal which for the thermistors is $P_r = 10$ mW, and for the barretter is $P_r = 1.0$ mW. Fig. 4 shows similar measurements for the Schottky diode. The level of the reference signal for the Schottky-diode measurements is $P_r = 0.1$ mW. Fig. 4 also shows the changes that occur as the modulation frequency is increased from 0.1 to 10 kHz. These changes are due to the $1/f$ noise characteristics and the frequency response of the 1:4 step-up transformer.

The dynamic range of the detectors in this report is defined as

$$Ad = 10\log(P_r/P_m) \tag{15}$$

where P_r is the reference power level, and P_m is the modulated signal power level that produces a 3-dB signal-to-noise ratio at the input to the vector voltmeter. Fig. 5 shows a plot of Ad versus P_r for the three different detectors at 2 GHz. If the detectors are truly "square law," then Ad increases by 20 dB for every 10-dB increase in P_r. The deviation from linearity in the Schottky-diode measurement is caused by the diode's deviation from square law.

A summary of the dynamic range observed during the tests is given in Table I. The reference level P_r in this summary is 10 mW for the thermistor, 1.0 mW for the barretter, and 0.1 mW for the diode. These reference levels are all chosen as being typical of the maximum power that the three detectors are subjected to in normal six-port measurements.

IV. Modulated Six-Port Measurement System

An experimental, dual six-port network analyzer was modified for the subcarrier modulation technique as shown in Fig. 6 [6]. Basically, four isolators, a bi-phase modulator, and a low-pass filter are added ahead of six-port number 2. The low-pass filter after the bi-phase modulator insures

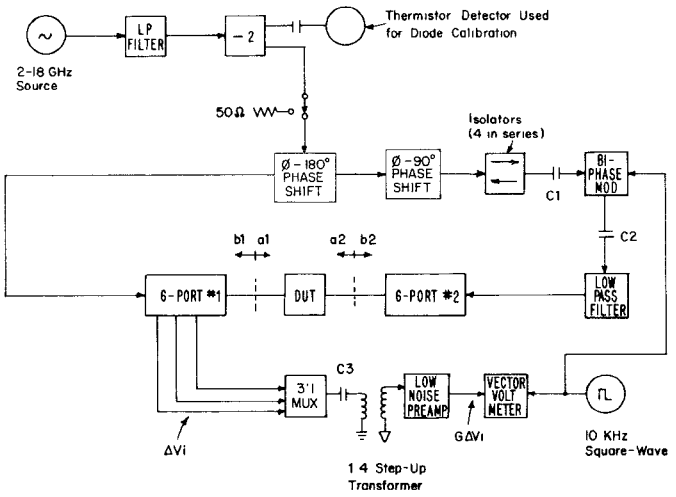

Fig. 6. Block diagram of dual six-port automatic network analyzer with modifications for modulation technique.

that any harmonics generated by this unit are attenuated by at least 80 dB relative to the fundamental. Capacitors C1 and C2, as in the previous experiment, are inner and outer dc blocks that are used to suppress 10-kHz ground loops. The detected output from each of the diodes in six-port 1 is sent to a 3:1 multiplexer which then selects one of the signals for amplification in the 1:4 step-up transformer and low-noise preamplifier. After amplification, the voltage of the 10-kHz subcarrier is measured by the vector voltmeter. All of the modifications to the network analyzer are made so that measurements can be made with either the 10-kHz subcarrier or with the conventional unmodulated technique.

It is necessary, at this point, to reexamine some of the mathematics. First, let the voltage (peak-to-peak) of the 10-kHz square wave at the output of the ith diode be given by ΔV_i. The rms voltage measured at the vector voltmeter is related to the voltage at the diode by

$$M_i = G\Delta V_i \tag{16}$$

where G is a constant.

Previous work with the diode six-ports describes a function

$$P_i = F_i(V) \tag{17}$$

that relates the power P_i at the input of the ith diode to the dc voltage at the output of the diode [7]. The small power change at the ith diode, to a very good approximation, is given by

$$\Delta P_i \cong dP_i = \Delta V_i \left.\frac{d(F_i(V))}{dV}\right|_{V=V_i}. \tag{18}$$

Substituting (16) and (18) into (11) results in

$$S_{12} = \frac{1}{\alpha P_4 G\Delta\phi} \sum_{i=1}^{3} C_i M_i \left.\frac{d(F_i(V))}{dV}\right|_{V=V_i}. \tag{19}$$

V. Modulated Six-Port Calibration

Two different methods were used to calibrate the network analyzer for measurements with the modulation technique. Ideally, both methods should provide the same measurement accuracy. In reality, one method provides slightly better measurement accuracy because of system imperfections such as RF leakage, harmonics, etc.

For calibration method A, it is convenient to substitute

$$A = \alpha G\Delta\phi \tag{20}$$

into (19), yielding

$$S_{12} = \frac{1}{AP_4} \sum_{i=1}^{3} C_i M_i \left.\frac{d(F_i(V))}{dV}\right|_{V=V_i}. \tag{21}$$

All of the quantities except A in (21) are either measured directly or are obtained from the normal six-port and diode calibration [6], [8]. However, A can be obtained by simply measuring a known S_{12} and solving (21). A calibrated 60-dB attenuator is used as the known S_{12}. This attenuator, therefore, becomes a standard in the sense that all future measurements are relative to its "calibrated" value. It is important to note that the constants C_i are determined from the normal six-port calibration, which means the bi-phase modulator is in the off (zero degree) position. Thus, system imperfections caused by the modulator may not be present when the C_i are determined.

For calibration method B, (19) is rewritten as

$$S_{12} = \frac{1}{P_4} \sum_{i=1}^{3} E_i M_i \left.\frac{d(F_i(V))}{dV}\right|_{V=V_i} \tag{22}$$

where

$$E_i = \frac{C_i}{A}. \tag{23}$$

The E_i can be determined by measuring three known S_{12} and solving a linear set of simultaneous equations for E_i. The three known S_{12} were obtained by using the calibrated 60-dB attenuator, the calibrated 60-dB attenuator with a 6-cm precision air line in series, and the calibrated 60-dB attenuator with a 7.5-cm precision air line in series. Thus, with calibration method B, the three constants E_i are determined with the bi-phase modulator on. Calibration method B currently provides slightly better measurement accuracy. However, it is also more cumbersome in terms of the number of connections and disconnections required of the operator.

VI. Measurement Results

The modified network analyzer was tested by measuring various attenuators with S_{12} between -60 dB and -100 dB at 3 GHz. These attenuators are composed of two cascaded attenuators whose individual scattering parameters have been measured on the conventional unmodulated network analyzer. Fig. 7 shows the precision σ in the measurement of $|S_{12}|$, where σ is one standard deviation as observed during five repeat measurements. The precision of the network analyzer in the conventional, unmodulated,

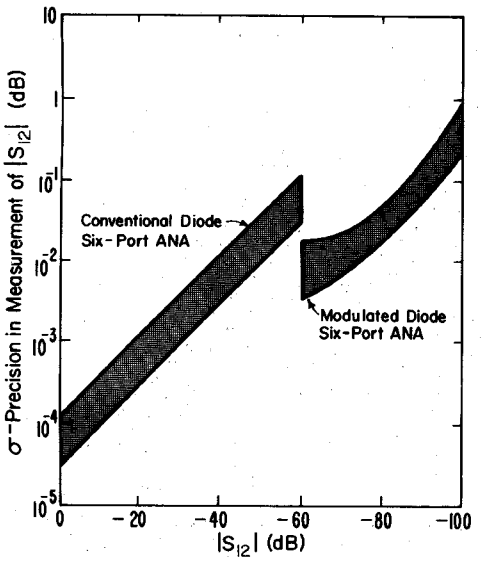

Fig. 7. Precision of measurements versus $|S_{12}|$. Measurement frequency is 3 GHz.

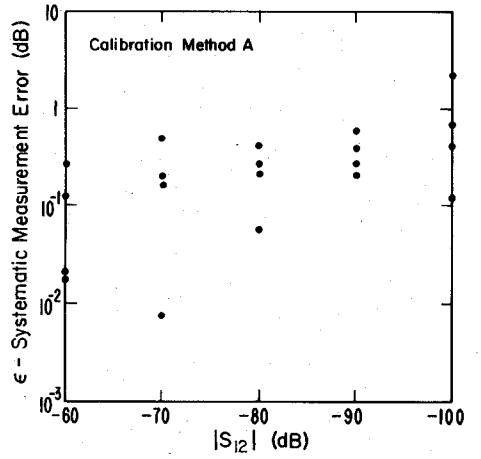

Fig. 8. Systematic measurement error versus $|S_{12}|$ using calibration method A. Measurement frequency is 3 GHz.

mode is also shown. Note that the precision in measuring $|S_{12}| = -80$ dB is 0.05 dB or better with the modulated network analyzer. No difference in precision was observed between the two different calibration methods.

The systematic error in the measurement of $|S_{12}|$ is defined as

$$\epsilon \left| |S_{12}| - |S_{12}|_{\text{true}} \right| \tag{24}$$

where $|S_{12}|$ is the measured value, and $|S_{12}|_{\text{true}}$ is the estimated true value obtained by cascading the scattering parameters of the individual attenuators. A plot of the systematic error versus $|S_{12}|$ is shown in Fig. 8 for calibration method A and Fig. 9 for calibration method B. The systematic errors in measuring 80-dB attenuators are of the order of 0.4 dB or less using calibration method A and 0.16 dB or less using method B.

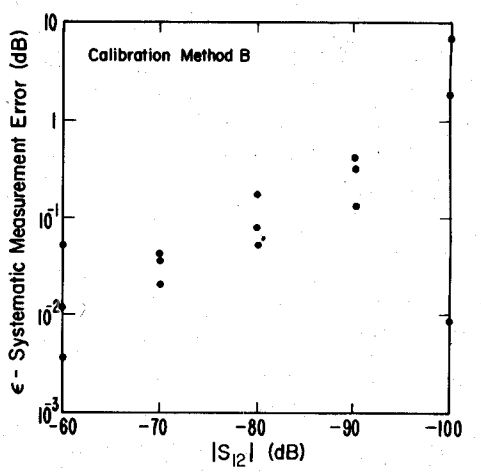

Fig. 9. Systematic measurement error versus $|S_{12}|$ using calibration method B. Measurement frequency is 3 GHz.

VII. Conclusions

The modulation technique provides a significant improvement in the measurement capabilities of the diode network analyzer. Measurements of 80-dB attenuators can be consistently made with a precision of 0.05 dB or better. Unfortunately, the systematic errors are somewhat greater. Systematic errors in measuring 80-dB attenuators are as large as 0.4 dB using calibration method A, and 0.16 dB using calibration method B. A significant engineering effort is still required to develop a standards quality system for measuring $|S_{12}|$ greater than 60 dB. Some of the problems that still need to be addressed are as follows.

a) Radio frequency leakage from the diodes, connector, modulator, etc., is significant and must be reduced for quality measurements.

b) The effects of errors from harmonics generated by the diode power detectors and the diode bi-phase modulator need to be evaluated.

c) The four isolators that precede the bi-phase modulator and the 3-GHz filter that follows it are narrowband. Ideally, all components of the network analyzer should be as wideband as possible.

d) The discrepancies in measurements using calibration method A versus B need to be resolved. It is anticipated that these discrepancies will disappear as the other sources of errors such as harmonics and RF leakage are removed.

e) The current technique is dependent on the gain stability of the vector voltmeter. No method currently exists, other than recalibration, for detecting any gain changes in this unit.

f) The physical packaging of the six-ports needs to be carefully evaluated if measurements of $|S_{12}|$ greater than 80 dB are to be consistently made. Problems with rigidity, temperature stability, RF leakage, etc., must be addressed.

Appendix A

The ANA can be thought of as a three-port network whose ports consist of the two measurement ports 1 and 2, and one port for the generator input, port 3. Let s_{ij} be the

s-parameter of this three-port network. Then one can derive the following from the three-port scattering equations:

$$\frac{a_2}{a_1} = H_3 \frac{1 - H_1\Gamma_1}{1 - H_2\Gamma_2} \tag{A1}$$

where

$$H_3 = s_{23}/s_{13} \tag{A2}$$

$$H_2 = s_{22} - s_{12}H_3 \tag{A3}$$

and

$$H_1 = s_{11} - s_{21}/H_3. \tag{A4}$$

The reflection coefficients Γ_1 and Γ_2 measured by the two six-ports can be written in terms of the S-parameter of the device under test S_{ij} and of a_2/a_1 as

$$\Gamma_1 = S_{11} + S_{12}a_2/a_1 \tag{A5}$$

$$\Gamma_2 = S_{22} + S_{21}a_1/a_2. \tag{A6}$$

When measuring devices with loss greater than 60 dB, $|S_{12}|$ will be less than 0.001. For the other parameters, reasonable estimates are

$$|a_2/a_1| = 1$$

$$|S_{11}| = |S_{22}| = 0.1$$

and

$$|S_{13}| = |S_{23}| = 0.3.$$

Thus, (A5) and (A6) can be approximated as

$$\Gamma_1 = S_{11} \tag{A7}$$

$$\Gamma_2 = S_{22}. \tag{A8}$$

These approximations reduce (A1) to

$$\frac{a_2}{a_1} = H_3 \frac{1 - H_1S_{11}}{1 - H_2S_{22}}. \tag{A9}$$

Expanding $1/(1 - H_2S_{22})$ in a power series in H_2S_{22}, one can write (A9) as

$$\frac{a_2}{a_1} = H_3(1 - H_1S_{11} + H_2S_{22} + \cdots). \tag{A10}$$

When the phase shifter is changed to the second phase position, a_2/a_1 changes to

$$\frac{a_2'}{a_1'} = H_3'(1 - H_1'S_{11} + H_2'S_{22} + \cdots). \tag{A11}$$

The change in a_2/a_1 is the difference between (A10) and (A11)

$$\Delta\phi \equiv \frac{a_2}{a_1} - \frac{a_2'}{a_1'} = H_3 - H_3' - S_{11}(H_3H_1 - H_3'H_1') + S_{22}(H_3H_2 - H_3'H_2') + \cdots. \tag{A12}$$

The magnitude of the first terms $H_3 - H_3'$ on the right of (A12) is a constant whose magnitude is approximately 2. Using estimates of the s_{ij} above, one can show that the magnitude of the remaining terms in (A12) are considerably less than 2, showing that $\Delta\phi$ is essentially a constant.

Appendix B

An expression relating $|a_1|^2$ and P_4 may be obtained by considering six-port 1 and its detectors as a three-port consisting of output port 1, port 4, and the input to the six-port which we will call port 0. Let σ_{ij} be the S-parameters of this three-port network where $i, j = 0, 1, 4$. Then one can derive an equation similar to (A1) from the three-port scattering equations

$$\frac{a_4}{a_1} = D_3 \frac{1 - D_1\Gamma_1}{1 - D_2\Gamma_4} = D_4(1 - D_1\Gamma_1) \tag{B1}$$

where

$$D_4 = D_3/(1 - D_2\Gamma_4)$$

$$D_3 = \sigma_{40}/\sigma_{10} \tag{B2}$$

$$D_2 = \sigma_{44} - \sigma_{14}D_3 \tag{B3}$$

$$D_1 = \sigma_{11} - \sigma_{41}/D_3 < 0.1. \tag{B4}$$

Note that D_4 is a constant independent of the device under test. As in Appendix A, we can let $\Gamma_1 = S_{11}$ for high-loss pads. Then (B1) leads to

$$P_4 \propto |a_1|^2|1 - D_1S_{11}|^2.$$

Substituting estimates of the σ_{ij} in (B4), one can show that

$$|D_1S_{11}| \ll 1$$

for reasonably well-matched pads. Then P_4 is proportional to $|a_1|^2$, which is the desired result.

Acknowledgment

The authors would like to acknowledge the contributions of J. Yehle in constructing the measurement system and preparing the software for the tests.

References

[1] C. A. Hoer, "A network analyzer incorporating two six-port reflectometers," *IEEE Trans. Microwave Theory Tech.*, vol. MTT-25, pp. 1070–1074, Dec. 1977.

[2] C. A. Hoer, "Using six-port and eight-port junctions to measure active and passive circuit parameters," *Nat. Bur. Stand. (U.S.) Tech. Note 673*, pp. 10, Sept. 1975.

[3] R. J. King, *Microwave Homodyne Systems*. London, England: Peter Peregrinus Ltd., 1978, pp. 78–100.

[4] N. T. Larsen, "A new self-balancing dc-substitution rf power meter," *IEEE Trans. Instrum. Meas.*, vol. IM-25, pp. 343–347, Dec. 1976.

[5] N. T. Larsen and F. R. Claque, "The NBS type II power measurement system," *Adv. Instrum.*, vol. 25, pt. 3, paper 712-70, in *Proc. 25th Annual ISA Conf.* (Philadelphia, PA), Oct. 26–29, 1970.

[6] J. R. Juroshek and C. A. Hoer, "A dual six-port network analyzer using diode detectors," *IEEE Trans. Microwave Theory Tech.*, vol. MTT-32, pp. 78–82, Jan. 1984.

[7] C. A. Hoer, K. C. Roe, and C. M. Allred, "Measuring and minimizing diode detector nonlinearity," *IEEE Trans. Instrum. Meas.*, vol. IM-25, pp. 324–329, Dec. 1976.

[8] G. F. Engen and C. A. Hoer, "Thru-reflect-line: An improved technique for calibrating the dual six-port automatic network analyzer," *IEEE Trans. Microwave Theory Tech.*, vol. MTT-25, pp. 1070–1074, Dec. 1977.

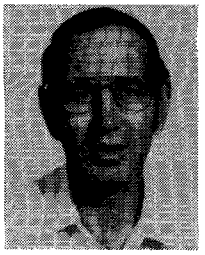

John R. Juroshek was born in Sheridan, WO, on January 7, 1940. He received the B.S. and M.S. degrees in electronic engineering from the University of Wyoming, Laramie, in 1961 and 1962, respectively. In 1966, he attended the University of California, Berkeley, for a year of postgraduate study in communications theory.

From 1962 to 1963, he was employed with the Federal Aviation Agency. In 1963, he joined the staff of the Department of Commerce at Boulder, CO. Since that time, he has worked with the Institute of Telecommunication Sciences and the National Bureau of Standards in various areas of communications, antenna research, propagation research, and system design. His present interests are in automated systems and automated network analyzers.

✠

Cletus A. Hoer (S'66–M'67) was born in Westphalia, MO, in 1933. He attended Weber State College, Ogden, UT, and Sophia University, Tokyo, Japan, while serving in the U.S. Air Force from 1950 to 1954. He received the B.S. degree in engineering physics and the M.S. degree in electrical engineering, both from the University of Colorado, Boulder, in 1959 and 1967, respectively.

He joined the Boulder Laboratories, National Bureau of Standards, Boulder, CO, in 1956, where he was first engaged in developing instrumentation for measuring properties of magnetic materials at high frequencies. In 1962, he transferred to the High Frequency Impedance Standards Section, where he did research and development work on inductance standards, impedance bridges, inductive voltage dividers, attenuators, and directional couplers.

In 1972, his emphasis shifted to developing Josephson junction detectors for precision RF attenuation measurements. Since 1974, he has been working on the theory and application of the six-port concept to RF and microwave measurements. He and a co-worker, Glenn Engen, received the Department of Commerce Gold Medal Award, in 1976, for their development of the six-port concept. He is presently the leader of the Microwave Metrology Group at NBS and is the author or co-author of 40 technical papers and holds two patents.